2-Dihydromethylpiperazinediium-M^{II} (M^{II} = Cu^{II}, Fe^{II}, Co^{II}, Zn^{II}) double sulfates and their catalytic activity in diastereoselective nitroaldol (Henry) reaction

Houcine Naïli,*[a] Fadhel Hajlaoui,[a] Tahar Mhiri,[a] Tatiana C. O. Mac Leod,[b] Maximilian N. Kopylovich,[b] Kamran T. Mahmudov[b] and Armando J. L. Pombeiro*[b]

A series of double dihydromethylpiperazinediium metallic sulfates **1–7** [H$_2$mpz]M^{II}(SO$_4$)$_2$·nH$_2$O (mpz = 2-methylpiperazine, C$_5$H$_{12}$N$_2$) are prepared by slow evaporation using a racemic (*R/S*)-mpz (for **1**, **2**) or enantiopure *R*-mpz (for **3**), *S*-mpz (for **4–7**) and sulfates of Cu^{II} (for **5**), Fe^{II} (for **1**, **4**), Co^{II} (for **7**) and Zn^{II} (for **2**, **3**, **6**), and characterized by infrared spectroscopy, elemental analysis and single crystal X-ray diffraction. The [M^{II}(H$_2$O)$_6$]$^{2+}$, [(*R/S*)-H$_2$mpz]$^{2+}$, [(*R*)-H$_2$mpz]$^{2+}$ or [(*S*)-H$_2$mpz]$^{2+}$ cations and 2SO$_4$$^{2-}$ anions are linked together *via* two types of hydrogen bonds, Ow–Hw⋯O and N–H⋯O, leading to supramolecular arrangements. The use of the racemic 2-mpz provides alternatives in crystallization: a centrosymmetric structure where the enantiomers are related by an appropriate crystallographic symmetry operation or one where the enantiomers occupy the same crystallographic position, generating disorder. Compounds **1–7** act as diastereoselective catalysts for the nitroaldol (Henry) reaction. The diastereoselectivity can be regulated from exclusive *threo* to exclusive *erythro* isomer preparation with typical yields of 50–99%, depending on the catalyst and the substrate used.

Introduction

The chemistry of organically templated metal sulfates is a rapidly expanding research field due to their structural diversities and potential applications as functional materials.[1–3] For instance, the double sulfates of divalent metal and chiral organic amines exhibit interesting ferroelectric or non-linear optical properties such as frequency doubling or second harmonic generation.[4,5] The use of optically pure organic compounds as catalysts in stereoselective organic transformations is another currently growing area of research.[6–10] Recently a lot of publications appeared where enantiopure organics are combined with metal ions in complex catalysts combining stereo-specificity of the former with the high activity of the latter. In particular, several chiral metal–organic frameworks (MOFs) were found to be highly regio- and stereo-selective for a number of useful chemical transformations.[7] Usually the preparation of such MOFs constitutes a rather complicated task, while the application of the easy to prepare M^{II}-complexes, composed of organic (*e.g.* aminium) and inorganic (metal ion)

cations and a sole anion, *e.g.* sulfate, is usually out of attention. Hence, it would be attractive to prepare and structurally characterize such mixed salts and demonstrate their stereo (diastereo) activity in a useful reaction.

The Henry or nitroaldol reaction (combination of nitroalkane and aldehyde, a very important synthetic tool for the creation of a carbon–carbon bond and up to two stereogenic centers) can be used as a model reaction to check the catalytic activity.[11–14] Usually this reaction is carried out in the presence of strong bases, leading to dehydration with concomitant formation of a nitroolefin. The interest in asymmetric versions of this reaction started growing after the work[15,16] on the use of chiral bimetallic lithium–lanthanum catalysts, whereby the control of stereochemistry of two newly generated carbon centres has become possible. In the last two decades many other asymmetric catalysts have been developed and nowadays aldehydes or α-keto esters can be converted to the corresponding nitroalkanol with good enantio- and diastereo-selectivity.[17–19] However, to our knowledge, salts containing jointly a metal and an asymmetric organic cation (*e.g.* 2-H$_2$mpz^{2+}) have not yet been applied as catalysts for this reaction.

Thus, the main aims of the current work are as follows: (i) to synthesize and structurally characterize the salts or the M^{II}-complexes (M^{II} = Fe, Co, Cu and Zn) containing either racemic or chiral 2-H$_2$mpz and different doubly charged metal

[a]Laboratoire de l'Etat Solide, Département de Chimie, Université de Sfax, BP 1171, 3000 Sfax, Tunisie. E-mail: houcine_naili@yahoo.com
[b]Centro de Química Estrutural, Complexo I, Instituto Superior Técnico, Technical University of Lisbon, Av. Rovisco Pais, 1049-001 Lisbon, Portugal. E-mail: pombeiro@ist.utl.pt

cations; (ii) to study the catalytic activity and diastereoselectivity of the synthesized salts in the nitroaldol combination of nitroethane with various aldehydes.

Results and discussion

Synthesis and characterization of the salts

Compounds $[(R/S)\text{-}C_5H_{14}N_2][Fe(H_2O)_6](SO_4)_2$ (**1**), $[(R/S)\text{-}C_5H_{14}N_2]$-$[Zn(H_2O)_6](SO_4)_2$ (**2**), $[(R)\text{-}C_5H_{14}N_2][Zn(H_2O)_6](SO_4)_2$ (**3**), $[(S)\text{-}C_5H_{14}N_2][Fe(H_2O)_6](SO_4)_2$ (**4**), $[(S)\text{-}C_5H_{14}N_2][Cu(H_2O)_6](SO_4)_2$ (**5**), $[(S)\text{-}C_5H_{14}N_2][Zn(H_2O)_6](SO_4)_2$ (**6**), $[(S)\text{-}C_5H_{14}N_2][Co(H_2O)_6]$-$(SO_4)_2$ (**7**) (see Fig. 1 and Table 1) were obtained by slow evaporation of water solutions containing metal(II) sulfates, sulfuric acid and either racemic or chiral cyclic diamine 2-methylpiperazine.[20–23] All the structures of **1**–**7** are related: the asymmetric units in each compound consist of organic cations, SO_4 tetrahedra and one M^{II} cation octahedrally coordinated to six oxygen atoms, all being held together through extensive hydrogen-bonding networks. However, the symmetries of the synthesized salts differ greatly. Compounds **1**–**2**, which were synthesized using racemic 2-mpz, crystallize in the centrosymmetric space groups $P2_1/n$ and $P2_1/c$. In contrast, salts **3**–**7**, prepared from enantiopure 2-mpz, crystallize in the noncentrosymmetric polar space group $P2_1$.

Description of X-ray crystal structures of compounds 1 and 2

1 and **2** (Fig. 1) are built from $[M^{II}(H_2O)_6]^{2+}$, $(SO_4)^{2-}$ and disordered $[H_2mpz]^{2+}$ ions linked together by an extensive three-dimensional H-bonding network similar to the related salts of cobalt, nickel and manganese.[21] The metal cations are located in special positions on crystallographic inversion centers and each is coordinated by six oxygen atoms from water molecules of which three are crystallographically independent. The 2-dihydromethylpiperazinediium cations are located about crystallographic inversion centers, with all atoms located in general positions. The $Fe(H_2O)_6$ and $Zn(H_2O)_6$ octahedra are slightly distorted. Bond angles O–Fe–O fall in the range [86.59(7)–93.41(7)°], while the O–Zn–O angles range from 86.15(6)° to 93.85(3)°. The intermolecular $M^{II}\cdots M^{II}$ distance in **1** is considerably longer than that found in **2** (7.083(2) Å and 6.599(2) Å, respectively), possibly attributed to the radii of metallic cations and the nature of disorder in the organic groups of **1** by comparison with **2**. Moreover, two disorder mechanisms are observed in the $[H_2mpz]^{2+}$ cations with two orientations of both $[(R)\text{-}H_2mpz]^{2+}$ and $[(S)\text{-}H_2mpz]^{2+}$ enantiomers. In compound **1** the organic cations are partly disordered (disorder in the carbon of methyl groups with the occupancy factor equal to 0.5), while in **2** the C and N atoms are distributed between two positions related by the symmetry centre with a refined site occupancy factor equal to 0.5. The disordered $[H_2mpz]^{2+}$ cations reside between the inorganic layers, balancing charge and participating in the extensive hydrogen-bonding network.

The sulfate anions are stacked such that they form anionic layers parallel to the cationic ones. They play an important role

in the stability of the crystal structures by linking the organic and inorganic cations *via* Ow–H⋯O and N–H⋯O hydrogen bonds. Within the intermolecular bonds, the N⋯O distances vary between 2.767(3) and 2.866(3) Å in **1** and between 2.664(2) and 2.910(3) Å in **2**. The Ow⋯O distances range from 2.694(3) to 2.810(2) Å and between 2.560(4) and 2.841(5) Å in **1** and **2**, respectively.

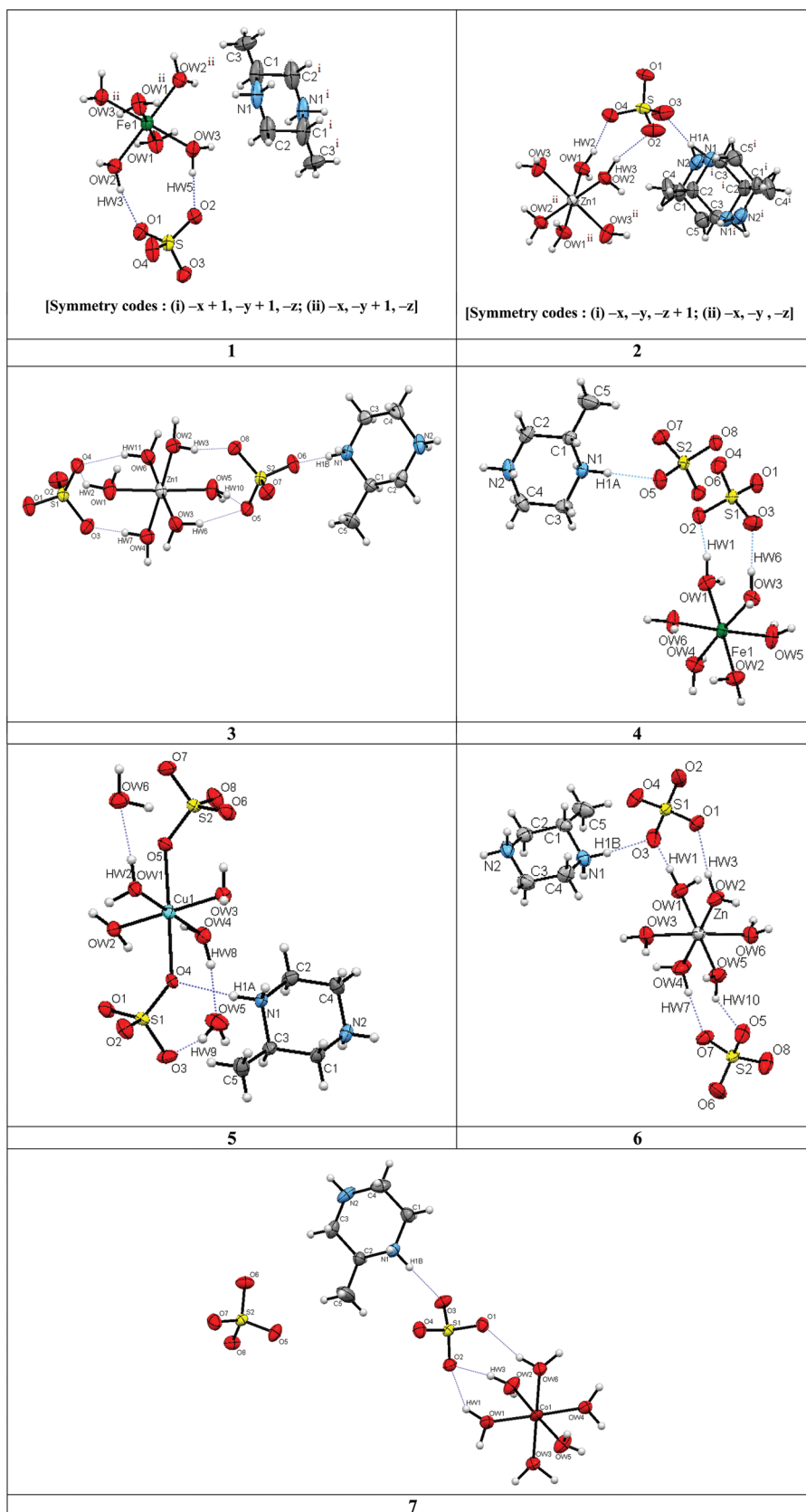### Description of X-ray crystal structures of compounds 3–7

Both structures and compositions are similar in salts **3**–**7** (Fig. 1). Each compound **3**, **4**, **6** and **7** contains a single unique divalent metal (M^{II} = Fe^{II}, Co^{II} or Zn^{II}), a chiral organic H_2mpz cation and two sulfate tetrahedra, all of which lie in general positions, while compound **5** consists of isolated tetraaquabis (sulfato-O) copper anions $[Cu(SO_4)_2(H_2O)_4]^{2-}$, organic cations $[(S)\text{-}H_2mpz]^{2+}$ and two free water molecules. The crystal structures belong to the polar, noncentrosymmetric space group $P2_1$, crystal class 2 ($C2$) for which the only symmetry elements are a series of 2_1 screw axes. The Flack parameters refined to −0.028(9), 0.020(9), 0.001(2), −0.015(11) and −0.013(13) for **3**, **4**, **5**, **6** and **7**, respectively.

The possibility of pseudosymmetry with the inorganic components of **3**–**7** was investigated. The organic cations were removed from the crystallographic models, and PLATON[30] was used to probe for missing symmetry. The ADDSYM command suggests the possibility of a missing additional symmetry leading to the $P2_1/c$ space group, with inversion symmetry directly between the metal centers.

The position of the methyl groups on the 2-methylpiperazinediium cation rings violates the pseudosymmetry found by PLATON, does not recognize the contribution of a single CH_3 group over the rest of the structures. In addition, the systematic absences are not correct for $P2_1/c$. Specifically, the expected l = $2n$ + 1 absences in $h0l$ reflections are not present. These results confirm the occurrence of a noncentrosymmetric space group and agree with the chemical pathway in which enantiomeric molecules have been used in compounds **3**–**7**.

The molecular arrangements are described by an alternation of cationic and anionic layers. The three-dimensional packing of **3**–**7** shows similar polyhedra with slight variation of them and the organic cations. The resulting H-bonding networks can be alternatively described by three-dimensional supramolecular frameworks belonging to three different structure types, forming channels in which the R or S-2-H_2mpz cations play a templating role. However, despite the similarities in compositions in compounds **3**–**7**, distinct differences in three-dimensional packing are observed between the Zn^{II} (**3** and **6**), Fe^{II} (**4**), Cu^{II} (**5**) and Co^{II} (**7**).[20,22,23]

Compounds **3**, **4**, **6** and **7** are all constructed from octahedrally coordinated transition metal cations coordinated by six water molecules $[M(H_2O)_6]^{2+}$, isolated sulfate anions $(SO_4)^{2-}$, and either $[(R)\text{-}H_2mpz]^{2+}$ or $[(S)\text{-}H_2mpz]^{2+}$ cations. The octahedra environments of M^{II} (M^{II} = Fe^{II}, Co^{II} and Zn^{II}) are not regular, as seen in other isostructural metal sulfates.[2–4] O–M^{II}–O bond angles range by the transition metal with averages of 87.05(8)°, 85.88(5)°, 86.87(1)° and 88.84(8)° observed for **3**, **4**, **6**

[Symmetry codes : (i) −x + 1, −y + 1, −z; (ii) −x, −y + 1, −z]

1

[Symmetry codes : (i) −x, −y, −z + 1; (ii) −x, −y, −z]

2

3

4

5

6

7

Fig. 1 Ellipsoid plots with an atom labeling scheme for **1–7** (ellipsoids are drawn at the 50% probability level).

Table 1 List of compounds studied in this work

Compound	Code	Space group	CCDC number	References
$[(R/S)\text{-}C_5H_{14}N_2][Fe(H_2O)_6](SO_4)_2$	1	$P2_1/c$	828001	21
$[(R/S)\text{-}C_5H_{14}N_2][Zn(H_2O)_6](SO_4)_2$	2	$P2_1/n$	859890	22
$[(R)\text{-}C_5H_{14}N_2][Zn(H_2O)_6](SO_4)_2$	3	$P2_1$	859888	22
$[(S)\text{-}C_5H_{14}N_2][Fe(H_2O)_6](SO_4)_2$	4	$P2_1$	823975	20
$[(S)\text{-}C_5H_{14}N_2][Cu(H_2O)_6](SO_4)_2$	5	$P2_1$	724064	23
$[(S)\text{-}C_5H_{14}N_2][Zn(H_2O)_6](SO_4)_2$	6	$P2_1$	859889	22
$[(S)\text{-}C_5H_{14}N_2][Co(H_2O)_6](SO_4)_2$	7	$P2_1$	823974	20

Scheme 1 Formation of nitroaldols by the Henry reaction.

and **7**, respectively. The $[M^{II}(H_2O)_6]^{2+}$ cations are separated from one another through the shorter distances, 5.359(2), 7.035(3), 6.582(3) and 7.091(3) Å. The organic cations $[(R)\text{-}H_2mpz]^{2+}$ or $[(S)\text{-}H_2mpz]^{2+}$ donate hydrogen bonds to neighboring $(SO_4)^{2-}$ tetrahedra. The N–H···O distances range between 2.673(3) and 2.913(3) Å, while the Ow–H···O range between 2.664(3) and 2.983(4) Å.
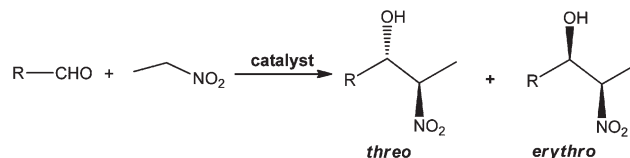
Compounds **3** and **6** are produced from enantiomeric components and interestingly crystallize with different chiral unit cells. Indeed, in the experiment, the concentration of sulfuric acid is crucial in the synthesis of complexes **3** and **6**. Surprisingly, the high acidity (pH 1–1.5) supports the formation of compound **3**, while low acidity increases the formation of **6**.

The crystal structure of $[(S)\text{-}H_2mpz][Cu(H_2O)_4](SO_4)_2 \cdot 2H_2O$ (**5**) consists of isolated $[Cu(SO_4)_2(H_2O)_4]^{2-}$ anions, $[(S)\text{-}H_2mpz]^{2+}$ cations and free water molecules linked together by two types of hydrogen bonds, N–H···O and Ow–H···O. The Cu^{II} atoms are coordinated by two oxygen atoms of sulfate groups and four corners of water molecules forming distorted octahedra geometry. The Cu^{II} ions in this complex display so-called [4 + 2] type of coordination that has often been observed, which is consistent with a Jahn–Teller distortion.[31] The O–Cu^{II}–O angles range from 88.75(1)° to 91.24(2)°. The intermetallic centres are isolated from one another with a shortest distance Cu···Cu = 7.558(2) Å. This $M^{II}···M^{II}$ distance in **5** is the longest one found in this work. Cooperative hydrogen bond networks are present. Indeed, the intermolecular distances N···O vary from 2.742(6) to 2.855(4) Å and the Ow···O range between 2.643(4) to 2.886(5) Å.

In the complexes **1–7**, the S–O distances range from 1.462(2) to 1.485(2) Å with an average of 1.473(2) Å. Slight differences in the S–O bond lengths together with the slight deformation of the anions reflect how the ionic radii of the M^{II} cations affect the supramolecular structures. The chemical formula of these materials resembles that of the Tutton's salts.[2,3] Indeed, although replacing monovalent metals by divalent organic cations, there are strong similarities between the two families, with difference resulting from the size, shape and charge of the amino group involved in the present structures.

Catalytic activity of 1–7 in the Henry reaction

To optimize the reaction (Scheme 1) conditions, we examined the association of benzaldehyde and nitroethane, varying the catalyst amount, time, temperature and solvent (Table 2). No

product formation was observed in the absence of the catalysts as well as in the presence of simple metal sulfates (Table 2, entries 14–19), while the application of **1–7** allows us to obtain mixtures of β-nitroalkanol diastereoisomers (*threo* and *erythro* forms) in high yields up to 98% and high enantiomeric excesses (up to 85% ee). **1** appears to be more active than the other tested compounds (Table 2, entry 1), but it is not very selective, while **3–7** demonstrate excellent diastereoselectivity towards the *erythro* or the *threo* isomer (Table 2, entries 3–7). The possible reasons for the different diastereoselectivity being influenced by (i) enantiomeric structures of the complexes R- (for **3**) and S- (for **4–7**); (ii) hydrogen bonding interactions between the protonated imino groups in the mpz (which can act as hydrogen bond donors) and the developing O in the transition state (which can accept a hydrogen bond). Such interactions could, if well organized, favor the formation of a given product *via* transition state stabilization. Next we have chosen **1** (due to its high activity), **3** (due to the *erythro* selectivity) and **5** (due to the *threo* selectivity) for further study.

As a preliminary solvent screening demonstrates, methanol is a better solvent than benzaldehyde or nitroethane, presumably due to a tighter ion pairing in the course of association with H-shift.[14] We have also examined the effect of other solvents (entries 8–13, Table 2). In the case of **1** the solvent polarity influences the selectivity, while for **3** and **5** no effect on the selectivity is observed. Generally, the yield depends on solvent polarity and low yields are obtained in less polar solvents, possibly due to low solubility of the catalysts.[14] Control reactions were carried out in the absence of catalysts **1–7** but in the presence of $ZnCl_2$, $Zn(SO_4)_2$, $Co(SO_4)_2$, $Fe(SO_4)_2$ or $Cu(SO_4)_2$ (entries 14–19, Table 2). There is no reaction between benzaldehyde and nitroethane in the absence of the metal complex, even in the presence of metal salts (entries 14–19, Table 2). Next the increase of the catalyst amount enhances the product yield from 96 to 98% (**1**), from 5 to 11% (**3**) and from 17 to 51% (**5**) for the respective amounts of 1 mol% and 3 mol% of these catalysts (entries 20–28, Table 2). The reaction was time-dependent. Decreasing the reaction time led to significant decrease in the conversion (entries 29–37, Table 2). There is not an effect to selectivity of the reaction on reducing the time. On the other hand, increasing the temperature in the 20–45 °C range not significantly improves the yield of β-nitroalkanol for 24 h reaction time (entries 38–43), as well as the selectivity of the reaction.

The reactions of a variety of *para-* (NO_2 or OCH_3) or *ortho-* (CH_3) substituted aromatic and aliphatic aldehydes with nitroethane (Table 3; **1** and **5** were used as the catalyst

Table 2 Catalytic activity of **1–7** in Henry reaction[a]

Entry	Catalyst	Time (h)	Amount of catalysts (mol%)	Temp (°C)	Solvent	Yield[b] (%)	Selectivity[c] threo/erythro
1	**1**	24	2.0	20	MeOH	97.4	73 : 27
2	**2**	24	2.0	20	MeOH	46.7	81 : 19
3	**3**	24	2.0	20	MeOH	6.54	0 : 100
4	**4**	24	2.0	20	MeOH	46.2	100 : 0
5	**5**	24	2.0	20	MeOH	49.9	100 : 0
6	**6**	24	2.0	20	MeOH	40.8	100 : 0
7	**7**	24	2.0	20	MeOH	37.0	100 : 0
8	**1**	24	2.0	20	THF	59.0	48 : 52
9	**3**	24	2.0	20	THF	5.25	0 : 100
10	**5**	24	2.0	20	THF	23.3	100 : 0
11	**1**	24	2.0	20	MeCN	32.1	65 : 35
12	**3**	24	2.0	20	MeCN	5.74	0 : 100
13	**5**	24	2.0	20	MeCN	37.4	100 : 0
14	Blank	24	—	20	MeOH	—	—
15	$ZnCl_2$	24	1.0	20	MeOH	—	—
16	$Zn(SO_4)_2$	24	1.0	20	MeOH	—	—
17	$Co(SO_4)_2$	24	1.0	20	MeOH	—	—
18	$Fe(SO_4)_2$	24	1.0	20	MeOH	—	—
19	$Cu(SO_4)_2$	24	1.0	20	MeOH	—	—
20	**1**	24	1.0	20	MeOH	95.8	72 : 28
21	**1**	24	3.0	20	MeOH	98.2	73 : 27
22	**1**	24	4.0	20	MeOH	98.2	72 : 28
23	**3**	24	1.0	20	MeOH	4.61	0 : 100
24	**3**	24	3.0	20	MeOH	11.3	0 : 100
25	**3**	24	4.0	20	MeOH	11.5	0 : 100
26	**5**	24	1.0	20	MeOH	17.4	100 : 0
27	**5**	24	3.0	20	MeOH	51.2	100 : 0
28	**5**	24	4.0	20	MeOH	51.6	100 : 0
29	**1**	5	3.0	20	MeOH	42.1	72 : 28
30	**1**	10	3.0	20	MeOH	69.2	73 : 27
31	**1**	15	3.0	20	MeOH	87.3	73 : 27
32	**3**	5	3.0	20	MeOH	3.5	0 : 100
33	**3**	10	3.0	20	MeOH	6.7	0 : 100
34	**3**	15	3.0	20	MeOH	9.3	0 : 100
35	**5**	5	3.0	20	MeOH	22.2	100 : 0
36	**5**	10	3.0	20	MeOH	35.4	100 : 0
37	**5**	15	3.0	20	MeOH	44.7	100 : 0
38	**1**	24	3.0	35	MeOH	99.1	73 : 27
39	**1**	24	3.0	45	MeOH	99.3	72 : 28
40	**3**	24	3.0	35	MeOH	13.6	0 : 100
41	**3**	24	3.0	45	MeOH	14.0	0 : 100
42	**5**	24	3.0	35	MeOH	55.7	100 : 0
43	**5**	24	3.0	45	MeOH	57.3	100 : 0

[a] Reaction conditions: 1.0–4.0 mol% (0.1–0.4 μmol) of a catalyst precursor (typically 2 mol%), solvent (MeOH, THF, MeCN) (2 mL), nitroethane (4 mmol) and benzaldehyde (1 mmol). [b] Determined by ^{1}H NMR analysis (see Experimental). [c] Calculated by ^{1}H NMR.

precursor) were also studied and shown to provide the respective β-nitroalkanols with yields ranging from 35 to 99% and with selectivities up to 100% for the *threo* isomer. The nature of substrates greatly influences the yields and selectivities. Hence, the electron-withdrawing group (NO_2) leads to lower yields compared with those for the electron-donating OCH_3 moiety (entries 3 and 4 *vs.* 5 and 6, Table 3). In the case of 2-methylbenzaldehyde, low selectivity and yield are observed, probably due to steric hindrance (entries 7 and 8, Table 3). For aliphatic aldehydes, a good yield is observed for acetaldehyde the shortest one (entries 9–12).

Moreover, *p*-substituents on the aromatic ring of aldehyde enhanced enantioselectivity, exhibiting nearly exclusive formation of *anti*-diastereomers with 39–54% ee (entries 1, 3 and 5). The reaction of aldehyde with the electron-withdrawing –NO_2 group proceeded smoothly (entry 7), whereas the
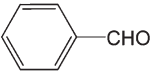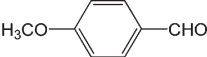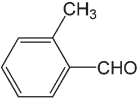
sluggish reactions were observed in the reaction of aldehyde with the *p*-methoxy substituent (entry 5).

Conclusions

The directed synthesis of noncentrosymmetric double dihydromethylpiperazinediium metallic sulfates was achieved through the incorporation of the enantiomerically pure chiral amine 2-methylpiperazine. Despite the presence of crystallographic disorder when using a racemic source of the amine, the syntheses containing either *S* or *R*-2-mpz result in five noncentrosymmetric compounds. The thus synthesized salts [H_2mpz]-$M^{II}(SO_4)_2 \cdot n H_2O$ can be used as effective (isolated yields up to 99%) and selective catalysts of the nitroaldol addition between aromatic aldehydes and nitroethane in a methanol medium,

Table 3 Henry reaction of various aldehydes and nitroethane with catalysts **1** and **5**[a]

Entry	Substrate	Catalyst	Yield[b] (%)	*Threo/erythro* ratio[c]	ee(anti)[d] (%)
1	(benzaldehyde, C_6H_5CHO)	**1**	97.4	73 : 27	47
2		**5**	49.9	100 : 0	82
3	(O_2N-benzaldehyde)	**1**	83.2	65 : 35	39
4		**5**	35.4	100 : 0	77
5	(H_3CO-benzaldehyde)	**1**	98.5	78 : 22	54
6		**5**	53.8	100 : 0	85
7	(2-methylbenzaldehyde, CH_3)	**1**	79.7	75 : 25	52
8		**5**	27.3	100 : 0	81
9	CH_3CHO	**1**	99.1	76 : 24	52
10		**5**	58.4	100 : 0	78
11	CH_3CH_2CHO	**1**	98.7	72 : 28	43
12		**5**	52.1	100 : 0	76

[a] Reaction conditions: 2.0 mol% of catalysts **1** (derived from racemic *R/S*-mpz) and **5** (derived from chiral *S*-mpz), methanol (2 mL), nitroethane (4 mmol) and benzaldehyde (1 mmol), reaction time: 24 h. [b] Determined by ^1H NMR analysis (see Experimental). [c] Calculated by ^1H NMR. [d] Determined by chiral HPLC analysis.

in contrast with some previously reported results in other systems.[11–19,24,25] The isolated yields of the final products depend on structural limitations and solvent polarity. Catalyst **3** is selective towards the *erythro* isomer, whereas **5** to the *threo* one. Thus, comparison of the activities of **5** with those of other catalysts[11–19,24,25] indicates that the former has a promising potential towards the Henry diastereoselective transformation, being, to our knowledge, among the most selective (100%) towards the *threo* isomer so far reported for the nitroaldol reaction under mild conditions.

Experimental section

Materials

$FeSO_4·7H_2O$ (99%, Merck), $ZnSO_4·7H_2O$ (99%, Merck), $CoSO_4·7H_2O$ (99%, Merck), $CuSO_4·5H_2O$ (99%, Merck), 2-methylpiperazine (95%, Aldrich), (*R*)-(−)-2-methylpiperazine (99%, Aldrich), (*S*)-(+)-2-methylpiperazine (99%, Aldrich) and H_2SO_4 (96%, Carlo Erba) and deionized water were used in the syntheses. Infrared spectra (4000–400 cm^{-1}) were recorded on a BIO-RAD FTS 3000MX instrument in KBr pellets. The ^1H and ^{13}C NMR spectra were recorded at ambient temperature on a Bruker Avance II + 300 (UltraShield™ Magnet) spectrometer operating at 300.130 and 75.468 MHz for proton and carbon-13, respectively. The chemical shifts are reported in ppm using tetramethylsilane as the internal reference. Carbon, hydrogen, and nitrogen elemental analyses were carried out by the Microanalytical Service of the Technical University of Lisbon. Electrospray mass spectra (ESI-MS) were run with an ion-trap instrument (Varian 500-MS LC Ion Trap Mass Spectrometer) equipped with an electrospray ion source. For electrospray ionization, the drying gas and flow rate were optimized according to the particular sample with 35 p.s.i. nebulizer pressure. Scanning was performed from *m/z* 100 to 1200 in a methanol solution. The compounds were observed in the positive mode (capillary voltage = 80–105 V).

Synthesis

The compounds were synthesized by slow evaporation from aqueous solutions.

$[(R/S)-H_2mpz][Fe(H_2O)_6](SO_4)_2$ (**1**) or $[(S)-H_2mpz][Fe(H_2O)_6]$-$(SO_4)_2$ (**4**): 0.2779 g (1.00 × 10^{-3} mol) $FeSO_4·7H_2O$ with 0.1000 g (1.00 × 10^{-3} mol) 2-mpz, 0.2128 g (2.17 × 10^{-3} mol) H_2SO_4, and 4.9500 g (2.75 × 10^{-1} mol) of deionized water were mixed under stirring for 15 min and left for slow evaporation. Dark green prismatic crystals started to form after a few days. Anal. calcd for $C_5H_{26}FeN_2O_{14}S_2$ (M = 458.24): C, 13.11; H, 5.72; N, 6.11. Found: C, 13.21; H, 5.61; N, 5.89. MS (ESI): *m/z*: 459.3 [M + H]$^+$. IR data (cm^{-1}): N–H 1463, 1634; C–H 3014; S–O 1094, 1195; O–H 3356.

$[(R/S)-H_2mpz][Zn(H_2O)_6](SO_4)_2$ (**2**), $[(R)-H_2mpz][Zn(H_2O)_6]$-$(SO_4)_2$ (**3**) or $[(S)-C_5H_{14}N_2][Zn(H_2O)_6](SO_4)_2$ (**6**) were synthesized similarly by joint evaporation of 0.2875 g (1.00 × 10^{-3} mol) of $ZnSO_4·7H_2O$, 0.1000 g (1.00 × 10^{-3} mol) of 2-mpz, 0.1962 g (2.00 × 10^{-3} mol) of H_2SO_4, and 4.9860 g (2.77 × 10^{-1} mol) of deionized water giving white prismatic crystals. Anal. calcd for $C_5H_{26}ZnN_2O_{14}S_2$ (M = 467.77): C, 12.84; H, 5.60; N, 5.99. Found: C, 12.74; H, 5.51; N, 5.49. MS (ESI): *m/z*: 468.3 [M + H]$^+$. IR data (cm^{-1}): N–H 1451, 1634; C–H 3012; S–O 1098, 1110; O–H 3344.

$[(S)-H_2mpz][Cu(H_2O)_4](SO_4)_2·2H_2O$ (**5**) was synthesized similarly from 0.2496 g (1.00 × 10^{-3} mol) of $CuSO_4·5H_2O$, 0.3000 g (3.00 × 10^{-3} mol) of *S*-2-mpz, 0.2265 g (2.31 × 10^{-3} mol) of H_2SO_4, and 4.9140 g (2.73 × 10^{-1} mol) of water giving blue prismatic crystals. Anal. calcd for $C_5H_{26}CuN_2O_{14}S_2$ (M = 465.94): C, 12.89; H, 5.62; N, 6.01. Found: C, 12.76; H, 5.41; N, 5.89. MS (ESI): *m/z*: 466.8 [M + H]$^+$. IR data (cm^{-1}): N–H 1457, 1511; C–H 3017, S–O 1097, 1221; O–H 3421.

$[(S)\text{-}C_5H_{14}N_2][Co(H_2O)_6](SO_4)_2$ (**7**) was synthesized from 0.2811 g (1.00×10^{-3} mol) of $CoSO_4 \cdot 7H_2O$, 0.3000 g (3.00×10^{-3} mol) of S-2-mpz, 0.2168 g (2.21×10^{-3} mol) of H_2SO_4, and 5.0040 g (2.78×10^{-1} mol) of water yielding red prismatic crystals. Anal. calcd for $C_5H_{26}CoN_2O_{14}S_2$ ($M = 461.33$): C, 13.02; H, 5.68; N, 6.07. Found: C, 12.93; H, 5.53; N, 5.94. MS (ESI): m/z: 462.2 $[M + H]^+$. IR data (cm^{-1}): N–H 1507, 1496; C–H 3020; S–O 1091, 1186; O–H 3432.

X-ray structure determinations

The X-ray quality single crystals of complexes **1**–**7** were immersed in cryo-oil, mounted on a Nylon loop and measured at a temperature of 293 K. Intensity data were collected using a Bruker AXS-KAPPA APEX II diffractometer with graphite monochromated Mo-Kα (λ 0.71073) radiation. Data were collected using omega scans of 0.5° per frame and full sphere of data was obtained. Cell parameters were retrieved using Bruker SMART software and refined using Bruker SAINT[26a] on all the observed reflections. Analytical absorption corrections were performed by modelling the crystal faces.[26b]

Structures were solved by direct methods by using the SHELXS–97 package[27] and refined with SHELXL–97.[28] Calculations were performed using the WinGX System–Version 1.80.03.[29] The aqua H atoms were located in a difference map and refined with O–H distance restraints of 0.96(1) Å and H–H restraints of 1.50(1) Å so that the H–O–H angle fitted to the ideal value of a tetrahedral angle. H atoms bonded to C and N atoms were positioned geometrically and allowed to ride on their parent atoms, with C–H and N–H bonds fixed at 0.97 and 0.90 Å, respectively.

Least squares refinements with anisotropic thermal motion parameters for all the non-hydrogen atoms and isotropic for the remaining atoms were employed. CCDC 828001 (**1**), 859890 (**2**), 859888 (**3**), 823975 (**4**), 724064 (**5**), 859889 (**6**), 823974 (**7**) contain the supplementary crystallographic data for this paper.

1: $M = 458.24$, monoclinic, space group $P2_1/c$, $a = 10.9273(2)$ Å, $b = 7.8620(10)$ Å, $c = 11.7845(3)$ Å, $\beta = 116.733(10)°$, $V = 904.20(3)$ Å^3, $Z = 2$, $D_{calc} = 1.683$ g cm^{-3}, $F_{000} = 480$, $\mu = 1.133$ mm^{-1}, 13 422 reflections collected, 2290 unique ($R_{int} = 0.0431$), $R_1 = 0.0540$, w$R_2 = 0.1156$ ($I > 2\sigma$).

2: $M = 467.77$, monoclinic, space group $P2_1/n$, $a = 5.5988(1)$ Å, $b = 10.9613(2)$ Å, $c = 12.5479(2)$ Å, $\beta = 101.3850(1)°$, $V = 889.75(3)$ Å^3, $Z = 2$, $D_{calc} = 1.746$ g cm^{-3}, $F_{000} = 488$, $\mu = 1.684$ mm^{-1}, 30 251 reflections collected, 3918 unique ($R_{int} = 0.0446$), $R_1 = 0.0502$, w$R_2 = 0.1288$ ($I > 2\sigma$).

3: $M = 467.77$, monoclinic, space group $P2_1$, $a = 10.8665(2)$ Å, $b = 7.8600(1)$ Å, $c = 11.7029(2)$ Å, $\beta = 116.2830°$, $V = 896.22(3)$ Å^3, $Z = 2$, $D_{calc} = 1.733$ g cm^{-3}, $F_{000} = 488$, $\mu = 1.672$ mm^{-1}, 10 529 reflections collected, 3957 unique ($R_{int} = 0.0482$), $R_1 = 0.0302$, w$R_2 = 0.0784$ ($I > 2\sigma$).

4: $M = 458.24$, monoclinic, space group $P2_1$, $a = 10.9444(4)$ Å, $b = 7.8602(3)$ Å, $c = 11.8020(4)$ Å, $\beta = 116.170(2)°$, $V = 911.19(6)$ Å^3, $Z = 2$, $D_{calc} = 1.670$ g cm^{-3}, $F_{000} = 480$, $\mu = 1.124$ mm^{-1}, 20 839 reflections collected, 8255 unique ($R_{int} = 0.0345$), $R_1 = 0.0471$, w$R_2 = 0.0880$ ($I > 2\sigma$).

5: $M = 465.94$, monoclinic, space group $P2_1$, $a = 7.5583(5)$ Å, $b = 10.1721(6)$ Å, $c = 10.7974(7)$ Å, $\beta = 94.425(4)°$, $V = 827.67(9)$ Å^3, $Z = 2$, $D_{calc} = 1.870$ g cm^{-3}, $F_{000} = 486$, $\mu = 1.646$ mm^{-1}, 24 878 reflections collected, 6454 unique ($R_{int} = 0.0463$), $R_1 = 0.0452$, w$R_2 = 0.1033$ ($I > 2\sigma$).

6: $M = 467.77$, monoclinic, space group $P2_1$, $a = 6.5819(2)$ Å, $b = 11.0014(2)$ Å, $c = 12.5229(3)$ Å, $\beta = 101.489(1)°$, $V = 888.62(4)$ Å^3, $Z = 2$, $D_{calc} = 1.748$ g cm^{-3}, $F_{000} = 488$, $\mu = 1.686$ mm^{-1}, 11 777 reflections collected, 3808 unique ($R_{int} = 0.0358$), $R_1 = 0.0384$, w$R_2 = 0.1003$ ($I > 2\sigma$).

7: $M = 461.33$, monoclinic, space group $P2_1$, $a = 10.8707(5)$ Å, $b = 7.8521(3)$ Å, $c = 11.7389(5)$ Å, $\beta = 116.3950(1)°$, $V = 897.55(7)$ Å^3, $Z = 2$, $D_{calc} = 1.725$ g cm^{-3}, $F_{000} = 514$, $\mu = 1.272$ mm^{-1}, 10 290 reflections collected, 4319 unique ($R_{int} = 0.0309$), $R_1 = 0.0379$, w$R_2 = 0.0982$ ($I > 2\sigma$).

Catalytic activity studies

A typical reaction was carried out under air as follows: to 1.0–4.0 mol% (0.1–0.4 µmol) of a catalyst precursor (typically 2 mol%) contained in the reaction flask were added methanol (2 mL), nitroethane (4 mmol) and aldehyde (1 mmol), in that order. The reaction mixture was stirred for the required time at room temperature and air atmospheric pressure. After evaporation of the solvent, the residue was dissolved in DMSO-d_6 and analyzed by ^{1}H NMR. The yield of the β-nitroalkanol product (relatively to the aldehyde) was established typically by taking into consideration the relative amounts of these compounds, as given by ^{1}H NMR and previously reported.[24,25] The adequacy of this procedure was verified by repeating a number of ^{1}H NMR analyses in the presence of 1,2-dimethoxyethane as an internal standard, added to the DMSO-d_6 solution, which gave yields similar to those obtained by the above method. Moreover, the internal standard method also confirmed that no side products were formed. The ratio between the *threo* and *erythro* isomers was also determined by ^{1}H NMR spectroscopy. In the ^{1}H NMR spectra, the values of vicinal coupling constants (for the β-nitroalkanol products) between the α-N–C–H and the α-O–C–H protons identify the isomers, being $J = 7$–9 or 3.2–4 Hz for the *threo* or *erythro* isomers, respectively.[24,25] The enantiomeric excess was determined by HPLC using a Shimadzu high performance liquid chromatograph with UV detection (210 nm). In the HPLC (OD-H, 4:96 isopropanol–hexane at 1 mL min^{-1}) four peaks at 35.1, 51.5 for the *anti* isomer and 43.9 and 57.1 for the *syn* isomer were observed.

Acknowledgements

access to the NMR facility, and IST Node of the Portuguese Network of mass-spectrometry (Dr Conceição Oliveira) for the ESI-MS measurements.

References

1 M. Dan, J. N. Behera and C. N. R. Rao, *J. Mater. Chem.*, 2004, **14**, 1257–1265.

2 S. Yahyaoui, W. Rekik, H. Naïli, T. Mhiri and T. Bataille, *J. Solid State Chem.*, 2007, **180**, 3560–3570.

3 C. N. Morimoto and E. C. Lingafelter, *Acta Crystallogr., Sect. B: Struct. Crystallogr. Cryst. Chem.*, 1970, **26**, 335–341.

4 L. F. Kirpichnikova, L. A. Shuvalov, N. R. Ivanov, B. N. Prasolov and E. F. Andreyev, *Ferroelectrics*, 1989, **96**, 313–317.

5 E. A. Muller, R. J. Cannon, A. N. Sarjeant, K. M. Ok, P. S. Halasyamani and A. J. Norquist, *Cryst. Growth Des.*, 2005, **5**, 1913–1917.

6 A. Berkessel, H. Gröger and D. MacMillan, *Asymmetric Organocatalysis – From Biomimetic Concepts to Applications in Asymmetric Synthesis*, Wiley-VCH, 2005, p. 454.

7 (*a*) H. Pellissier, *Recent Developments in Asymmetric Organocatalysis*, Springer, 2010, p. 241; (*b*) M. K. Bhunia, S. K. Das, M. M. Seikh, K. V. Domasevitch and A. Bhaumik, *Polyhedron*, 2011, **30**, 2218–2226.

8 F. Song, C. Wang and W. Lin, *Chem. Commun.*, 2011, **47**, 8256–8258.

9 D. Dang, P. Wu, C. He, Z. Xie and C. Duan, *J. Am. Chem. Soc.*, 2010, **132**, 14321–14323.

10 G. Nickerl, A. Henschel, R. Grünker, K. Gedrich and S. Kaskel, *Chem. Ing. Tech.*, 2011, **83**, 90–103.

11 G. Rosini, in *Comprehensive Organic Synthesis*, ed. B. M. Trost, I. Flemig, C. H. Heatcock, Pergamon, New York, 1991, vol. 2, pp. 321–340.

12 F. A. Luzzio, *Tetrahedron*, 2001, **57**, 915–945.

13 P. Hammar, T. Marcelli, H. Hiemstra and F. Himo, *Adv. Synth. Catal.*, 2007, **349**, 2537–2548.

14 M. N. Kopylovich, T. C. O. Mac Leod, K. T. Mahmudov, M. F. C. Guedes da Silva and A. J. L. Pombeiro, *Dalton Trans.*, 2011, **40**, 5352–5361.

15 H. Sasai, T. Suzuki, S. Arai and M. Shibasaki, *J. Am. Chem. Soc.*, 1992, **114**, 4418–4420.

16 M. Shibasaki and N. Yoshikawa, *Chem. Rev.*, 2002, **102**, 2187–2209.

17 C. Palomo, M. Oiarbide and A. Laso, *Eur. J. Org. Chem.*, 2007, 2561–2574.

18 J. Boruwa, N. Gogoi, P. P. Saikia and N. C. Barua, *Tetrahedron: Asymmetry*, 2006, **24**, 3315–3326.

19 C. Palomo, M. Oiarbide and A. Mielgo, *Angew. Chem., Int. Ed.*, 2004, **43**, 5442–5444.

20 F. Hajlaoui, H. Naïli, S. Yahyaoui, Alexander J. Norquist, T. Mhiri and T. Bataille, *J. Organomet. Chem.*, 2012, **700**, 110–116.

21 F. Hajlaoui, H. Naïli, S. Yahyaoui, M. M. Turnbull, T. Mhiri and T. Bataille, *Dalton Trans.*, 2011, **40**, 11613–11620.

22 H. Naïli, *J. Coord. Chem.*, 2012, **65**, 1178–1188.

23 F. Hajlaoui, S. Yahyaoui, H. Naïli, T. Mhiri and T. Bataille, *Inorg. Chim. Acta*, 2010, **363**, 691–695.

24 A. Cwik, A. Fuchs, Z. Hella and J. Clacens, *Tetrahedron*, 2005, **61**, 4015–4021.

25 V. J. Bulbule, V. H. Deshpande, S. Velu, A. Sudalai, S. Sivasankar and V. T. Sathe, *Tetrahedron*, 1999, **55**, 9325–9332.

26 (*a*) *Bruker, APEX2 & SAINT*, Bruker, AXS Inc., Madison, Wisconsin, USA, 2004; (*b*) J. De Meulenaer and H. Tompa, *Acta Crystallogr.*, 1965, **19**, 1014–1018.

27 G. M. Sheldrick, *Acta Crystallogr., Sect. A: Fundam. Crystallogr.*, 1990, **46**, 467–473.

28 G. M. Sheldrick, *Acta Crystallogr., Sect. A: Fundam. Crystallogr.*, 2008, **64**, 112–122.

29 L. J. Farrugia, *J. Appl. Crystallogr.*, 1999, **32**, 837–838.

30 A. L. J. Spek, *Appl. Crystallogr.*, 2003, **36**, 7–13.

31 V. M. Petrusevski, *Bull. Chem. Technol.*, 1990, **9**, 13–19.